ARTICLE OPEN

Check for updates

Decreased diffusivity along the perivascular spaces in bipolar disorder: an MRI-based cross-sectional and Mendelian randomization study

Zhuohui Chen[1,2,6,7]✉, Ziwei Teng[1,6], Yan Qiu[3], Sujuan Li[4], Xuelei Xu[4], Min Yang[4], Jindong Chen[1,4], Dong Yang[1,7]✉ and Hao Li[5,7]✉

The pathophysiology of bipolar disorder (BD) remains unclear. We investigated whether diffusion tensor imaging along perivascular spaces (DTI-ALPS), a putative MRI marker of glymphatic function, is altered in BD and whether this index relates to structural brain changes and clinical status. We recruited 108 patients with first-diagnosed and drug-naïve BD and 54 healthy controls. Participants underwent comprehensive clinical assessments (depression and mania ratings, functional disability, and neurocognition) and multimodal MRI (DTI-ALPS, free water [FW, a putative biomarker of neuroinflammation], FW-corrected mean diffusivity [MD-t], FW-corrected fractional anisotropy [FA-t], cortical thickness). We additionally assessed the causal association between DTI-ALPS and BD susceptibility using bidirectional Mendelian randomization (MR). BD patients exhibited reduced DTI-ALPS indices vs controls ($P = 0.004$), correlating with functional impairment (Sheehan Scale: P-corrected = 0.048) and executive dysfunction (Stroop Color and Word Test: P-corrected = 0.039). MR confirmed causal effects of lower DTI-ALPS on BD susceptibility (OR = 0.74, $P = 0.01$) without reverse causation. Lower DTI-ALPS indices were associated with higher FW in the forceps minor and inferior fronto-occipital fasciculus, and lower FA-t values in the forceps minor. Mediation analysis revealed that FW accumulation mediated 12.4% of the impact of alterations reflected by the DTI-ALPS index on executive performance. Together, these results provide convergent cross-sectional and genetic evidence that BD is associated with reduced DTI-ALPS, potentially reflecting impaired glymphatic fluid transport. These DTI-ALPS changes are clinically relevant, relating to disability and executive deficits in BD, and with increased FW, indicative of neuroinflammation, partly mediating this relationship.

Translational Psychiatry (2026)16:15 ; https://doi.org/10.1038/s41398-025-03753-1

INTRODUCTION

Bipolar disorder (BD), a psychiatric condition characterized by alternating episodes of mania and depression, remains incompletely understood in terms of its underlying mechanisms, posing significant challenges in diagnosis and treatment [1]. Previous postmortem histopathological studies have indicated that elevated neuroinflammation, as evidenced by increased lymphocyte infiltration [2] and high expression levels of interleukin (IL)-1 receptor and IL-1β mRNA, may contribute to the pathogenesis and progression of BD [3]. Considering the inflammatory factors and metabolic waste toxicity in BD, an efficient brain waste clearance system appears crucial for the prevention of disease progression and disease-related clinical disabilities.

Recent research has revealed the presence of a 'waste clearance' system within the central nervous system (CNS), known as the glymphatic system, which may be involved in the neuroinflammation in BD [4, 5]. In this system, cerebrospinal fluid (CSF) in the subarachnoid space flows into the brain's interstitial space through periarterial spaces and aquaporin-4 (AQP4) protein channels in astrocytic end-feet, mixes with interstitial fluid (ISF) and inflammatory factors, and ultimately drains through the perivenous spaces surrounding the deep medullary veins (Fig. 1) [6]. Therefore, glymphatic dysfunction may relate to the accumulation of inflammatory factors in several regions, resulting in brain damage and clinical deficits in patients with BD.

With the advance of MRI techniques, the diffusion tensor imaging along the perivascular space (DTI-ALPS) has emerged as a potential proxy for assessing glymphatic function in the brain [7, 8]. This index measures the diffusivity capacity of the perivenous space surrounding the deep medullary vein at the lateral ventricle body level, thus allowing for an assessment of the clearance capacity in the CSF outflow channel within the glymphatic system.

[1]Department of Psychiatry, The Second People's Hospital of Hunan Province (Hunan Brain hospital), Hunan University of Chinese Medicine, Clinical Research Center for Depressive Disorder in Hunan Province, 410021 Changsha, Hunan, China. [2]Department of Neurosurgery, Xiangya Hospital, Central South University, 87 Xiangya Road, Changsha 410008, China. [3]Xiamen Xianyue Hospital, Xianyue Hospital Affiliated with Xiamen Medical College, Fujian Psychiatric Center, Fujian Clinical Research Center for Mental Disorders, Xiamen 361012 Fujian, China. [4]National Clinical Research Center for Mental Disorders, Department of Psychiatry, China National Technology Institute on Mental Disorders, The Second Xiangya Hospital of Central South University, Changsha 410011 Hunan, China. [5]Department of Neurology, Radboud University Medical Center, Donders Institute for Brain, Cognition and Behavior, 6525 GA Nijmegen, The Netherlands. [6]These authors contributed equally: Zhuohui Chen, Ziwei Teng. [7]These authors jointly supervised this work: Zhuohui Chen, Dong Yang, Hao Li. ✉email: zhuohuichen0102@foxmail.com; youngdong@163.com; Hao.Li@radboudumc.nl

Received: 1 February 2025 Revised: 26 October 2025 Accepted: 7 November 2025
Published online: 19 November 2025

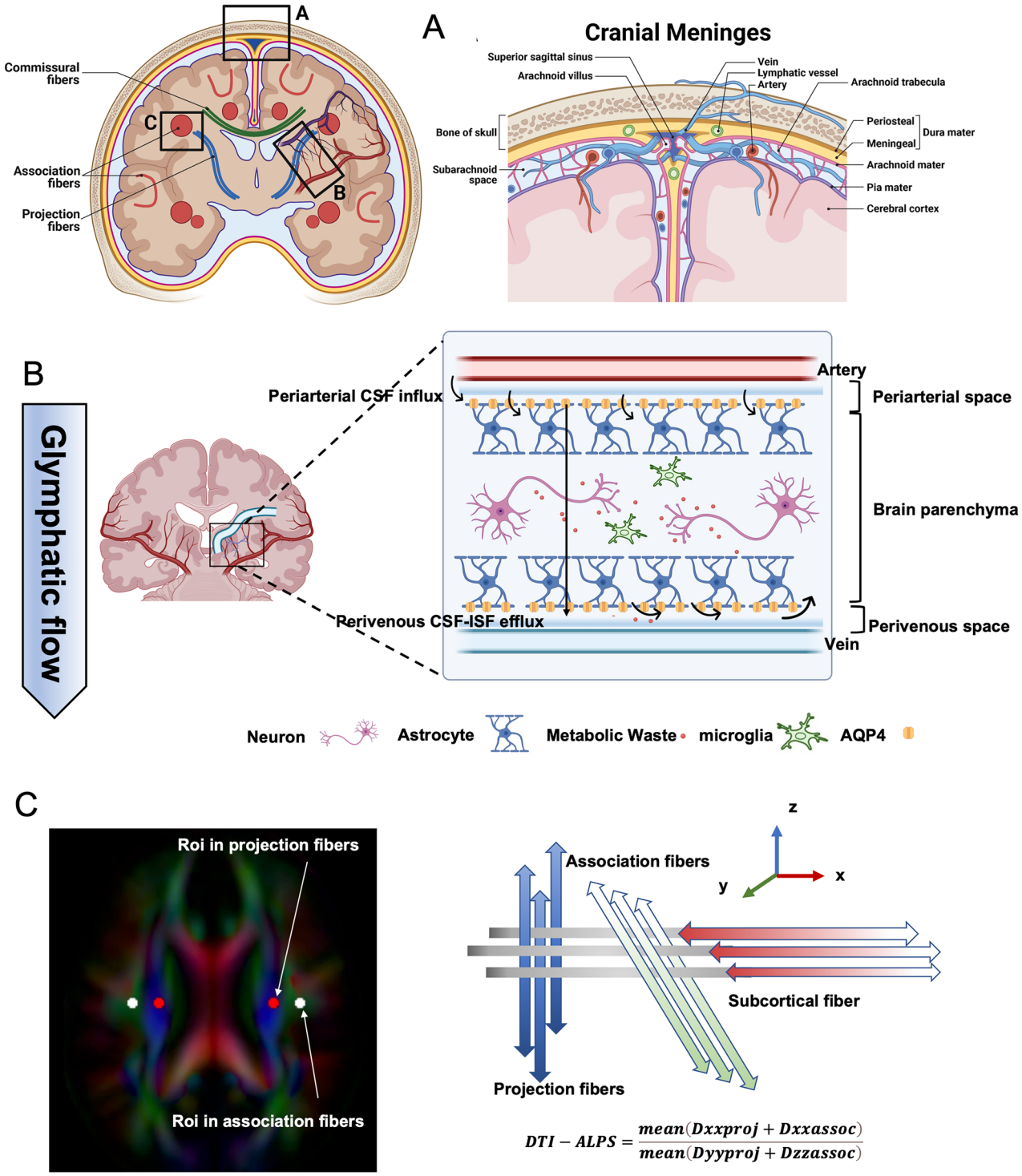

Fig. 1 Overview of glymphatic system on the macroscopic and microscopic scale. A The existence of meningeal lymphatic vessels and their relationship with surrounding vascular tissues indicate the existence of the lymphatic system in the brain. **B** The assumptive glymphatic function model. The cerebrospinal fluid (CSF) flows smoothly into the brain parenchyma from subarachnoid space, which is then drained out through perivenous spaces. During this process, the metabolic waste and inflammatory factors are also cleansed. **C** We exploited the DTI-ALPS index based on diffusion-weighted MRI as a proxy of glymphatic function. DTI-ALPS was computed as the ratio between the mean of the x-axis diffusivity on the projection fibres (Dxxproj) and association fibres (Dxxassoc) and the mean of the y-axis diffusivity on the projection fibres (Dyyproj) and the z-axis diffusivity on association fibres (Dzzassoc) in region of interest. DTI-ALPS, the diffusion along perivascular space. Images were created in BioRender. Teng, Z. (2025) https://BioRender.com/ye1q7xh.

Although not formally validated, DTI-ALPS has demonstrated a significant correlation with glymphatic clearance rates, as measured through invasive MRI with intrathecal gadolinium injection [9]. Recent cross-sectional studies have reported that patients with depression [10], schizophrenia [11], autism [12], and alcohol dependence [13], revealing a decreased DTI-ALPS and that is associated with a decline in cognitive function. However, evidence for DTI-ALPS changes in BD remains sparse.

In addition, observational studies are inherently limited in their ability to establish causality. Mendelian randomization (MR) analysis, by leveraging the wealth of available genome-wide association studies (GWAS), presents a powerful for elucidating the causal relationship between the exposures and outcomes [14, 15]. MR is grounded in Mendel's law of random assortment: genetic variants (i.e., single nucleotide polymorphisms [SNPs]) are randomly allocated at conception, thereby mimicking a process of randomized controlled trial. Because these variants are largely independent of environmental and lifestyle factors that confound observational studies, SNPs can be used as instrumental variables (IVs) to infer causality while minimizing confounding bias. Thus, MR can be applied to evaluate the potential causal relationship between DTI-ALPS and BD using relevant GWAS summary statistics [16].

Beyond DTI-ALPS, free water (FW) imaging derived from diffusion MRI quantifies the extracellular water fraction [17, 18]. Multiple studies have reported the increased FW in extensive regions of white and gray matter (GM) and related these increases with peripheral inflammatory markers in BD and schizophrenia [17, 19–21]. FW therefore represents a promising marker of neuroinflammation in psychiatric disorders, although increases may also reflect other pathological processes, such as vasogenic edema, axonal loss, or demyelination, that more commonly occur in cerebrovascular or neurodegenerative diseases [22, 23].

Despite these advances, no studies have evaluated cerebral glymphatic function using DTI-ALPS in patients with early-stage BD, and the relationships between this index, FW, and cerebral structural changes remain unclear. Therefore, this study aimed to: (1) investigate glymphatic dysfunction using the DTI-ALPS index in patients with first-diagnosed and drug-naïve BD. (2) investigate the causal relationships between DTI-ALPS index and BP using bidirectional MR. (3) assess DTI-ALPS index relationship with intracerebral FW, as well as the brain structural changes (i.e., cortical thickness and white matter [WM] microstructural integrity), and the clinical characteristics.

METHODS AND MATERIALS

Study participants

All patients and healthy controls were recruited from the Second Xiangya Hospital between 2019 March and 2022 February. The authors assert that all procedures contributing to this work comply with the ethical standards of the relevant national and institutional committees on human experimentation and with the Helsinki Declaration of 1975, as revised in 2013. All procedures involving human subjects/patients were approved by the Ethics Committee of the Second Xiangya Hospital of Central South University (approval number: 2018-067). All participants provided written informed consent. For children, we obtained additional written consent from their parents or legal guardians.

The inclusion criteria of the patients were: 1) age 16–50 years; 2) diagnosed with BD by at least two independent senior psychiatrists according to the Diagnostic and Statistical Manual of Mental Disorders, fifth edition criteria; 3) no prior diagnosis of any mental disorders; 4) absence of relevant medication history based on medical records and self-reported information; 5) Hamilton depression scale (HAM-D) scores 17 for patients with depressed-phase BD, Young Mania Rating Scale (YMRS) scores 12 for patients with manic- or hypomanic-phase BD, and meeting both standards for patients with mixed-phase BD. None of the patients had a history of active or chronic inflammatory diseases, organic brain disease, gout, renal disease, cardiovascular disease, other mental disorders, or any type of intellectual disability. Healthy controls of similar age, sex, and years of education with no previous history of illness or medication were also recruited.

Clinical, social role disability, cognitive, and executive function assessments

All patients underwent a detailed assessment of depression and mania severity using the HAM-D [24] and YMRS [25]. The Sheehan Disability Scale (SDS) [26] was used to assess three aspects of social role disabilities: work, social life, and family life disabilities. The Repeatable Battery for the Assessment of Neuropsychological Status (RBANS) Update was used to comprehensively assess five cognitive domains, namely immediate memory, visuospatial memory, language, attention, and delayed memory, based on 12 subitems. The compound score of each cognitive domain within the RBANS was calculated based on the corresponding sub-items and adjusted for age according to normative data. An additional cognitive domain, executive function, was assessed using the Stroop Colour and Word Test (SCWT) [27]. To ensure the consistency of the clinical evaluations, all assessing psychiatrists underwent standardized training to achieve a high level of inter-rater reliability in the administration and scoring of all rating scales.

MRI assessments

MRI was performed using a 3.0 T Philips Ingenia CX scanner (Philips Medical Systems) with standardised procedures for subject positioning under the following parameters: (1) sagittal 3D T1-weighted magnetization-prepared rapid gradient-echo (MP-RAGE): 1-mm isotropic voxels, repetition time (TR) = 8.111 ms, echo time (TE) = 3.705 ms, field of view (FOV) = 256 × 256 mm^2, flip angle = 7°, thickness = 1 mm; (2) single-shell diffusion using multi-band accelerated echo planar imaging (EPI): 30 diffusion-weighted directions (b = 1,000 s/mm^2), 2 × b = 0 images, 3-mm isotropic voxels, TR = 6000 ms, TE = 70 ms, FOV = 221 × 221 mm^2, and flip angle = 90°.

Diffusion MRI preprocessing

Diffusion MRI data were pre-processed to remove noise and Gibbs artefacts, correct head motion, eddy current-induced distortion, susceptibility-induced distortion (top-up), and intensity bias using MRtrix 3.0 software (version 3.0, http://www.mrtrix.org) [28], Functional Magnetic Resonance Imaging of the Brain Software Library (FSL; v6.0.3) software [29], Synb0-DISCO [30], and Advanced Normalisation Tools (ANTs, v 2.1.0) [31]. Due to the absence of a b0 image with reversed phase encoding in our DWI scans, 'topup' was performed based on a synthesised b0 image from the T1 image using Synb0-DISCO [30]. Next, with the pre-processed diffusion data, we calculated the mean diffusivity (MD) and fractional anisotropy (FA) maps of each participant using the 'dtifit' function within FSL [29].

Quantification of the DTI-ALPS

The DTI-ALPS index was calculated using a validated method, as described in previous study [9]. We placed four 5-mm-diameter spherical regions of interest (ROIs) in the bilateral projection and association fibres at the level of the lateral ventricular body using the ICBM-DTI-81 WM atlas [32]. Next, four ROIs in the ICBM template were registered to the individual's diffusion image using the 'fnirt' function within FSL. The positions of the registered ROIs were visually inspected. The DTI-ALPS index was computed using the following formula:

$$DTI-ALPS=\frac{mean(Dxxproj+Dxxassoc)}{mean(Dyyproj+Dzzassoc)}, \quad (1)$$

where *Dxxproj* is the ratio between the mean x-axis diffusivity on the projection fibres, *Dxxassoc* represents the association fibres, *Dyyproj* is the mean y-axis diffusivity on the projection fibres, and *Dzzassoc* represents the z-axis diffusivity on association fibres.

FW mapping

The DIPY (version 1.4.0, https://dipy.org/) Python package was used to fit a two-compartment model to the single-shell diffusion MRI data [18]. The model included a FW compartment (isotropic tensor with a fixed diffusion constant of water at 37 °C) and a tissue compartment (FW-corrected tensor). The estimated parameters were the fractional volume of the FW compartment (FW measure) and tensor of the tissue compartment. The FW measure expresses the relative contribution of FW in each voxel and ranges from 0 to 1. The tensor of the tissue compartment reflects the tissue microstructure after removing the signal constituted by FW, including the FW-corrected FA (FA-t) and FW-corrected MD (MD-t).

Surface-based analysis for cortical GM

GM abnormalities were investigated through surface-based vertex analyses using FreeSurfer software (version 7.3.2). To this end, T1W images were fed into the standard 'recon-all' processing pipeline within FreeSurfer to

reconstruct the cortical surface and estimate cortical thickness. The reconstructed surface was visually inspected, including the CSF/GM boundary (pial surface) and GM/WM boundary (WM surface), to ensure that there were no obvious errors in the reconstruction. The distance between pial and WM surfaces was measured to determine the cortical thickness map and was smoothed to improve the signal-to-noise ratio using a 10-mm full-width at half-maximum (FWHM) Gaussian kernel [33]. This smoothing size was chosen to balance the trade-off between reducing noise and preserving the spatial resolution of the surface-based cortical measurements [34].

The FW map was registered to the corresponding T1W image for each participant using the 'bbregister' function within FreeSurfer. The resulting FW map was then registered to the 'fsaverage' surface template and sampled along the cortex at a 50% depth from the pial surface to the WM surface using Freesurfer. We visually inspected the resampled cortical FW maps before smoothing with a 10-mm FWHM Gaussian kernel.

The cortical thickness and FW maps were used in the subsequent vertex-based analysis.

Tract-based spatial statistics for WM

To investigate WM abnormalities, FA images from all participants were input into the Tract-Based Spatial Statistics (TBSS) pipeline within the FMRIB software library (FSL, version 6.0.1), generating a mean FA image [29]. This image was subsequently skeletonised to produce a WM skeleton that represented common central tracts of the WM across all participants. Next, individual FW, FA-t, and MD-t images from each participant were projected onto the established WM skeleton. The aligned FW, FA-t, and MD-t maps obtained were used in subsequent voxel-wise analyses.

MR statistical analysis

This study utilized summary statistics for DTI-ALPS derived from the largest genome-wide association study (GWAS) of the UK Biobank Brain Imaging cohort (N = 31,021 individuals of European ancestry), as published by Huang et al [35]. Genetic association data for BD were sourced from the Psychiatric Genomics Consortium [36] (eTable 1). IVs were primarily defined as SNPs attaining genome-wide significance ($P < 5 \times 10^{-8}$). SNPs with an effect allele frequency (EAF) ≤ 0.01 were excluded in accordance with standard SNP inclusion criteria [37]. To ensure independence of IVs, linkage disequilibrium (LD) clumping was applied (LD threshold: $r^2 < 0.001$; clumping window: 10 Mb) using the European subset of the 1000 Genomes Project reference panel. Exposure and outcome datasets were harmonized, and palindromic SNPs with ambiguous allele frequencies were removed. The strength of IVs was assessed by calculating F-statistics for individual SNPs and average F-statistics for each trait, computed using the formula [38]:

$$F = \frac{R^2}{1-R^2} \times \frac{n-k-1}{k}$$

$$R^2 = \frac{\beta^2}{\beta^2 + se^2 \times n}$$

where n = sample size, k = number of IVs, R^2 = explained variance of genetic instruments on exposure, β = effect size of SNPs, and se = standard error of effect size

To minimize bias from weak instruments, all IVs included in MR analysis were restricted to those with F-statistics exceeding 10, thereby satisfying Assumption 1 of MR.

The primary analysis employed an inverse variance-weighted (IVW) approach with a multiplicative random-effects model, which aggregates Wald ratio estimates across individual IVs under the assumption that all genetic variants are valid instruments [39]. To evaluate the robustness of the results, supplementary methods were applied, including MR-Egger regression, weighted median, robust adjusted profile score (RAPS), and weighted mode estimators [40]. MR estimates were recalculated after excluding the outlier SNPs identified through MR- pleiotropy residual sum and outlier (PRESSO) [40]. Heterogeneity among genetic variants was assessed by generating funnel plots to visually inspect asymmetry and by calculating Cochran's Q statistic derived from the IVW method [41]. Sensitivity analyses included leave-one-out testing to determine whether the IVW estimates were unduly influenced by any single variant [42]. We evaluated genome-wide genetic correlation between the two traits (DTI-APLS and BD) using linkage disequilibrium score regression (LDSC). All analyses were conducted in R software (version 4.1.0) using the LDSC (version 1.0.1), TwoSampleMR (version 0.5.7) and MendelianRandomization packages.

Statistical analysis

Continuous variables were tested for normality using the Kolmogorov–Smirnov test, compared using Kruskal–Wallis test and are described as median (interquartile range, IQR). Categorical variables were compared using Fisher's exact test.

To determine whether patients with BD exhibit decreased DTI-ALPS values, an analysis of covariance (ANCOVA) was employed. This analysis compared DTI-ALPS values between patients with BD and HCs, as well as among the sub-group (three different phase include depressed-phase, mixed phase, manic-phase) of BD, while adjusting for age and sex. Furthermore, two linear regression models were applied in BD group to assess the effects of clinical severity on DTI-ALPS. In the two models, the HAM-D and YMRS scores were used as dependent variables, while DTI-ALPS values served as independent variables, adjusting for age, sex, and sub-group.

To examine the potential impact of DTI-ALPS on cerebral FW and structural abnormalities in BD, we performed vertex-wised analysis for GM and voxel-wised analysis for WM using Freesurfer and FSL softwares, respectively. For the GM, we employed two vertex-wise general linear models, in which we examined the vertex-wise associations between DTI-ALPS values, and cortical FW values or cortical thickness, respectively, while adjusting for age and sex. The false discovery rate method was employed to perform vertex-wise multiple comparisons within Freesurfer. For WM, we examined voxel-wise associations between DTI-ALPS values and WM measures (i.e., FW, FA-t, and MD-t), while adjusting for age and sex, by applying a permutation-based statistical interference tool for a non-parametric approach (5000 permutations). Threshold-free cluster enhancement-based (TFCE)-based wise error (FWE) correction was used for multiple comparisons. The mean FW, FA-t, and MD-t values of the regions that showed significant associations with the DTI-ALPS values were extracted and used in the subsequent analysis.

We employed linear regression models to examine the associations between DTI-ALPS and the clinical measures (i.e., SDS, RBANS, and SCWT) with different adjustments (model $1^{\&}$ and model $2^{\&}$). In model $1^{\&}$, adjustments were made for age, sex, and education years. In model $2^{\&}$, the sub-group was included as an additional adjustment to account for potential variations across disease periods. Note that, for RBANS cognitive scores (i.e., immediate memory, delayed memory, visuospatial, language and attention), age adjustment was not included in the regression models and the models were marked as model $1^{\#}$ and model $2^{\#}$. These scores were pre-adjusted for age using established normative datasets, making further age adjustment redundant. Mediation analyses were performed with the DTI-ALPS value as the initial variable, and the mean FW or FA-t values of the regions significantly associated with the DTI-ALPS value as the mediator, and the cognitive function and SDS score as the outcome variables. These mediation analysis models were adjusted for age, sex, and education and performed using the 'Mediation' package (version 4.5.0) in R. A 5000-bootstrap sampling was used to estimate the 95% confidence interval (CI).

Unless otherwise specified, all statistical analyses were performed using R software (version 4.1.0), and the significance level was set at a two-tailed P value < 0.05.

Supplementary analyses

Further analyses of group differences between BD and healthy controls, including TBSS of white matter FW, FA-t, and MD-t, as well as surface-based analyses of cortical thickness and cortical FW, are presented in the Supplementary Material ('Supplementary Method' section for method and 'Supplementary Results' section for results).

RESULTS

A total of 116 first-diagnosed, patients with drug-naïve BD and 55 healthy controls were included for assessment; eight patients with BD and one healthy control were excluded due to low-quality MRI images (n = 6) and image processing failure (n = 3). Finally, 108 patients with BD and 54 healthy controls were included. Age, sex, and education years were comparable between the two groups. The median HAM-D and YMRS scores in the patients were 23.0 and 10.0, respectively. The median SDS total score, work function, social life function, and family life function scores were 19.5, 7.0, 6.0, and 6.0, respectively. Compared with healthy controls, patients with BD showed significantly lower cognitive function scores for immediate memory, visuospatial function, language, attention, delayed memory, and executive functions (all P < 0.05).

Table 1. Demographic, clinical, social role, and cognitive characteristics of the study.

Characteristic	BD, N = 108[a]	HCs, N = 54[a]	*P*[b]
Age	20.0 (18.0, 22.0)	20.0 (19.3, 21.0)	0.38
Sex			0.46
Male	28 (25.9%)	17 (31.5%)	
Female	80 (74.1%)	37 (68.5%)	
Education years	14.0 (12.0, 16.0)	14.0 (14.0, 15.0)	0.82
Phase			
depressed	57 (52.8%)	–	
manic	11 (10.2%)	–	
mixed	40 (37.0%)	–	
HAM-D	23.0 (20.0, 28.0)	–	
YMRS	10.0 (5.0, 16.0)	–	
SDS total score[c]	19.5 (14.0, 23.0)	–	
Work function	7.0 (5.0, 8.0)	–	
Social life function	6.0 (5.0, 7.5)	–	
Family life function	6.0 (4.0, 8.0)	–	
RBANS total Index[d]	88.5 (82.0, 100.3)	103.0 (95.0, 113.0)	**<0.001*****
Immediate Memory Index	87.0 (77.0, 100.0)	104.0 (87.0, 112.0)	**<0.001*****
Visuospatial Index	85.0 (72.0, 97.0)	96.0 (87.0, 107.0)	**<0.001*****
Language Index	89.5 (82.8, 101.3)	101.0 (87.0, 107.5)	**0.011***
Attention Index	115.0 (106.0, 124.0)	120.0 (109.0, 131.3)	**0.024***
Delayed Memory Index	86.0 (81.0, 95.0)	97.0 (92.0, 105.0)	**<0.001*****
SCWT	40.0 (34.0, 46.0)	45.5 (40.0, 54.8)	**0.002****

BD bipolar disorder, *HCs* healthy controls, *SDS* Sheehan Disability Scale, *RBANS* Repeatable Battery for the Assessment of Neuropsychological Status Update, *SCWT* Stroop Color and Word Test.
**P*-uncorrected < 0.05. ***P*-uncorrected < 0.01. ****P*-uncorrected < 0.001.
[a]Median (IQR); n (%).
[b]Kruskal-Walli's rank sum test; Fisher's exact test.
[c]SDS is a self-rated scale measuring the social role function impairment in work, social, and family life.
[d]RBANS is composed of five cognitive domains which are already adjusted for age during the normalization.
Bold values are considered to indicate a statistically significant *P* value.

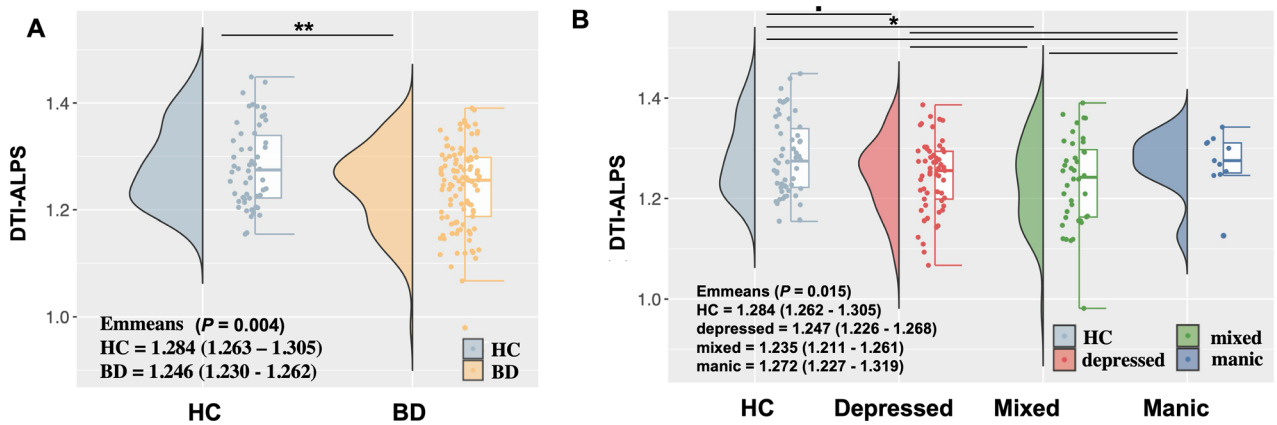

Fig. 2 DTI-ALPS index significantly reduced in patients with first-diagnosed and drug-naïve BD. A Violin plot for DTI-ALPS index in HCs and patients with BD. **B** Violin plot for DTI-ALPS index in HCs and different phases of BD. *P-corrected < 0.05; **P-corrected < 0.01. HCs, healthy controls; BD, bipolar disorder; DTI-ALPS, the diffusion along perivascular space.

Detailed clinical and demographic information is reported in Table 1 and eTable 2, respectively.

DTI-ALPS is significantly impaired in first-diagnosed, drug-naïve patients with BD

After adjusting for age and sex, patients with BD showed a significantly lower DTI-ALPS index than healthy controls ($P = 0.004$, $\eta 2 = 0.052$) (Fig. 2A). In the sub-group analyses, the differences between mixed-phase patients with BD and healthy controls remained significant (P-corrected < 0.05), but not for depressed-phase and manic-phase patients with BD (P-corrected > 0.05). No difference in the DTI-ALPS index was detected between the different clinical BD phases (Fig. 2B). Lower DTI-ALPS values were significantly associated with higher YMRS scores after

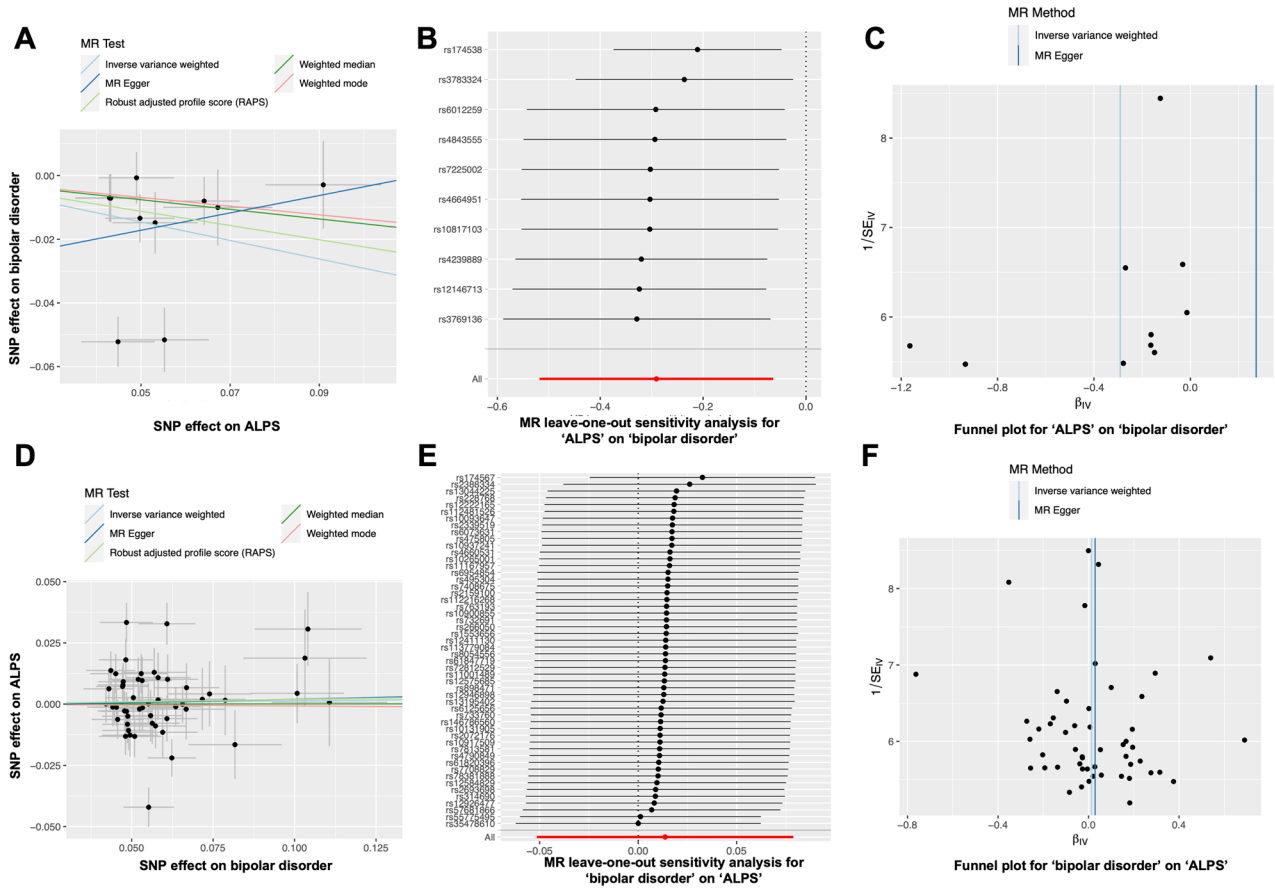

Fig. 3 The results of two-sample Mendelian randomization (MR) analysis between DTI-ALPS and BD. A Scatterplots for MR of DTI-ALPS on BD. **B** Leave-one-out plots for MR of DTI-ALPS on BD. **C** Funnel plots for MR of DTI-ALPS on BD. **D** Scatterplots for MR of BD on DTI-ALPS. **E** Leave-one-out plots for MR of BD on DTI-ALPS. **F** Funnel plots for MR of BD on DTI-ALPS. BD, bipolar disorder; DTI-ALPS, the diffusion along perivascular space.

adjusting age, sex, and phase (β = −0.116, P = 0.036, eTable 3). However, no significant association was found between the DTI-ALPS and HAM-D scores after adjusting for age, sex, and phase.

Bidirectional MR: changes in DTI-ALPS leading to BD

Following rigorous selection, 10 and 52 SNPs were retained for forward and reverse MR analyses, respectively. All selected SNPs demonstrated F-statistics >10, confirming their robustness as IVs (eTables 4, 5).

In forward MR analysis, the DTI-ALPS (IVW OR = 0.74, 95% CI = 0.59–0.93, P = 0.012) showed a negative association with the risk for BD (Fig. 3A, eTable 6). This finding was further corroborated by complementary analytical methods, including the weighted median method (OR = 0.86, 95% CI = 0.75–0.98, P = 0.027), RAPS (OR = 0.79, 95% CI = 0.66–0.96, P = 0.021), and PRESSO (OR = 0.87, 95% CI = 0.81–0.92, P = 0.003) test, all of which yielded consistent effect estimates (eTable 6). Leave-one-out analysis suggested that the MR estimate was not driven by a single SNP (Fig. 3B). The symmetry of the funnel plot indicated that there was no significant reporting bias, suggesting the reliability and robustness of the results (Fig. 3C). MR-Egger regression revealed no horizontal pleiotropy (all P > 0.05).

In reverse MR analysis, the BD (b = 0.014, 95% CI = 0.05–0.07, P = 0.68) showed no association with DTI-ALPS (Fig. 3D–F, eTable 7).

A non-significant LDSC result (P > 0.05, eTable 8) suggests no strong genome-wide genetic correlation between traits DTI-ALPS and BD, which means that the traits do not share widespread genetic variants across the genome and that the MR results were reliable.

Low DTI-ALPS indices correlated with local FW accumulation and WM microstructure lesion in first-diagnosed, drug-naïve patients with BD

The TBSS analysis showed that lower DTI-ALPS values were associated with higher FW values in specific regions, including the forceps minor, right inferior frontal-occipital fasciculus, left inferior longitudinal fasciculus, right uncinate fasciculus, and bilateral anterior thalamic radiation (P-corrected < 0.05), respectively (Fig. 4A and eTable 11). Additionally, we found an association between lower DTI-ALPS values and lower FA-t values in more concentrated regions, predominantly in the forceps minor (P-corrected < 0.05) (Fig. 4B, eTable 12). No significant associations were found between the DTI-ALPS and MD-t values. Furthermore, surface-based vertex analyses showed no association between DTI-ALPS and cortical thickness or FW values in the cortex.

Association between DTI-ALPS, cognitive function, and social role disability

For cognitive function, we found that higher DTI-ALPS index was associated with higher executive function scores while adjusting for age, sex and education (model 1[&]: β = 0.286, P-corrected = 0.039), but not with the scores in the other five cognitive domains (i.e., the immediate memory, visuospatial, language, attention, and delayed memory domain). The association between DTI-ALPS and executive function scores diminished after additional adjusting for phase (model 2[&]: β = 0.279, P-corrected = 0.054) (eTable 13). For social role disability, we found that higher DTI-ALPS was associated with the total lower SDS score while adjusting for age, sex, education and phase (model 2[&]:

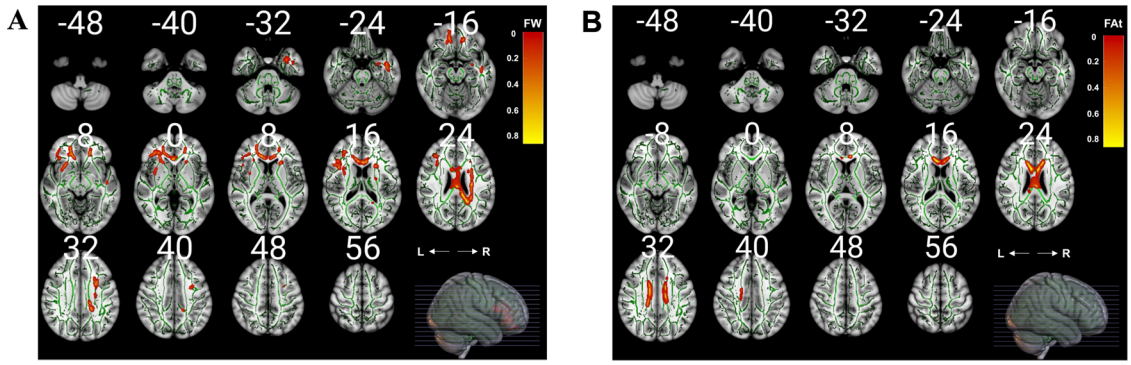

Fig. 4 Association of DTI-ALPS with free water and FA-t in white matter tracts. A TBSS analysis showed DTI-ALPS-related high-FW regions (P-corrected < 0.05, adjusted for age and sex) in patients with first-diagnosed drug-naïve BD. The coefficient of association (red to yellow) was drawn on top of the white matter skeleton (green) within the clusters mainly including forceps minor, inferior frontal-occipital fasciculus (R), inferior longitudinal fasciculus (L), uncinate fasciculus (R), and anterior thalamic radiation (L, R). TBSS: Tract-based spatial statistics. FW: free water. **B** TBSS analysis showed DTI-ALPS-related low-FA-t regions (P-corrected < 0.05, adjusted for age and sex) in patients with first-diagnosed drug-naïve BD. The coefficient of association (red to yellow) was drawn on top of the white matter skeleton (green) within the clusters, mainly including forceps minor. FA-t, fractional anisotropy of cellular tissue; TBSS, Tract-based spatial statistics; BD, bipolar disorder; DTI-ALPS, the diffusion along perivascular space.

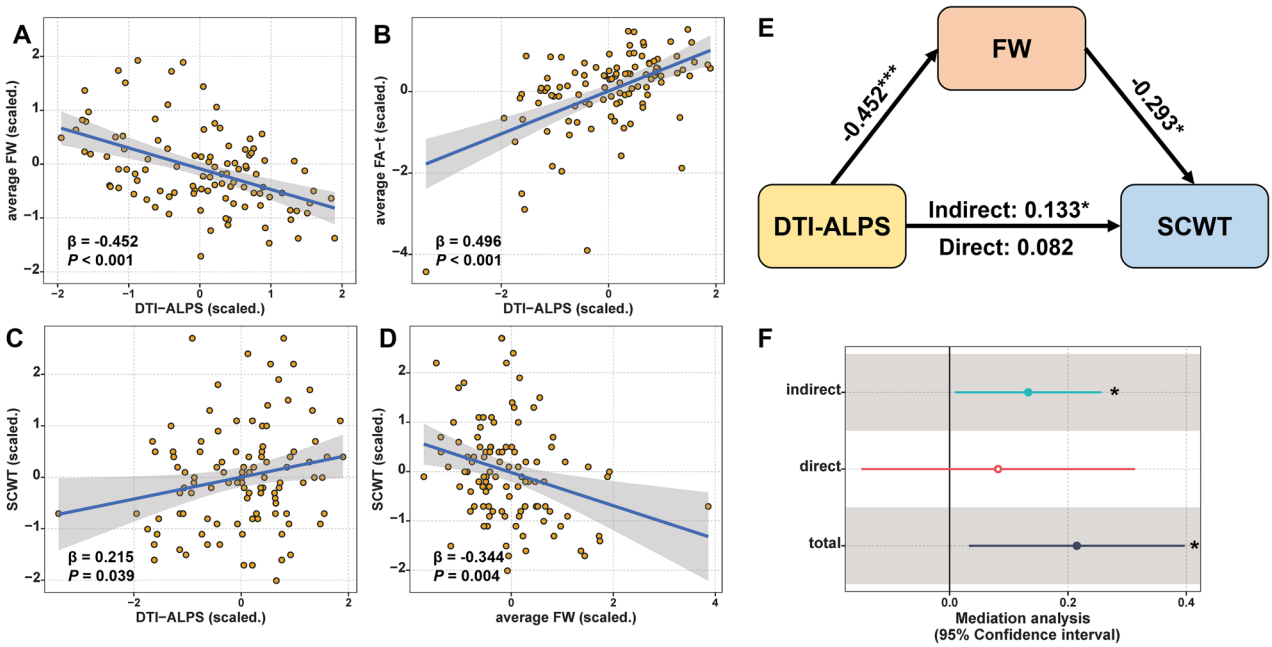

Fig. 5 The association between a reduced DTI-ALPS index and executive function impairment was mediated by FW elevation in patients with first-diagnosed and drug-naïve BD. A Multiple linear regression between DTI-ALPS and average FW while adjusting for age, sex, and education years. **B** Multiple linear regression between DTI-ALPS and average FA-t while adjusting for age, sex, and education years. **C** Multiple linear regression between DTI-ALPS and average SCWT while adjusting for age, sex, and education years. **D** Multiple linear regression between average FW and average SCWT while adjusting for age, sex, and education years. **E** Mediation analysis of FW in the relationship between DTI-ALPS and cognitive function proxied by SCWT. **F** The 95% CIs for indirect effects, direct effects, and total effects using bootstrapping of mediation models (n = 5000 samples). BD, bipolar disorder; DTI-ALPS, the diffusion along perivascular space; FW, free water; FA-t, fractional anisotropy of cellular tissue; SCWT, the Stroop Color and Word Test. *P-uncorrected < 0.05; **P-uncorrected < 0.01, ***P-uncorrected < 0.001.

β = −0.225, P-corrected = 0.048). In the sub-group analysis of the three SDS subitems (namely, family life, social life, and work disability), only the association between DTI-ALPS and family life disability remained significant, whereas the associations with the other two subitems did not. (eTable 14).

Further mediation analyses showed that the mean FW values of specific regions (identified in the TBSS analysis) mediated the association between DTI-ALPS and executive function (indirect effect = 0.133, P < 0.05) (Fig. 5). These regions included the forceps minor, right inferior frontal-occipital fasciculus, left inferior longitudinal fasciculus, right uncinate fasciculus, and bilateral anterior thalamic radiation regions. No mediation effect was found for FA-t values in the association between DTI-ALPS and any clinical measure.

DISCUSSION

In this study, we employed the DTI-ALPS index in the brain and assessed its association with cerebral FW accumulation, cerebral structural abnormalities, and clinical status in patients with first-diagnosed, drug-naïve BD. Our main findings were as follows: (1) patients with BD showed significantly lower DTI-ALPS values compared to healthy controls, with these decreases relating with the increased clinical severity (i.e., higher YMRS score); (2) MR

analysis showed the causal effect of DTI-ALPS on BD, while no reverse causal relationship was observed; (3) lower DTI-ALPS values were associated with higher FW and lower FA-t values in in specific regions, including the forceps minor, right inferior frontal-occipital fasciculus, left inferior longitudinal fasciculus, right uncinate fasciculus, and bilateral anterior thalamic radiation, and were also related to worse performances in cognition and social ability; (4) the association between DTI-ALPS values and executive function is mediated by FW accumulation of these WM region. Taken together, our findings showed that the decreased of DTI-ALPS contributed to FW accumulation in brain, which in turn contributed to the cognitive impairment and social dysfunction in BD.

We found that the patients with the newly diagnosed BD showed lower DTI-ALPS values compared with healthy controls, suggesting that glymphatic dysfunction may play a role in the early pathogenesis of BD. Although this index is not formally validated as the direct measurement of glymphatic function, it has demonstrated a significant correlation with glymphatic clearance rates, as measured through invasive MRI with intrathecal gadolinium injectionrecent [43]. Furthermore, extensive studies in various psychiatric conditions have reported a reduction in DTI-ALPS values, including depression [10], schizophrenia [44], autism spectrum disorder [12] and attention deficit hyperactivity disorder [45]. In addition, studies in in Alzheimer's Disease have reported that the decrease in DTI-ALPS was related to deposition of amyloid-β and tau protein [46]. These studies suggest that DTI-ALPS has the potential to serve as a marker for assessing the waste clearance capacity of the glymphatic system in the brain. However, its use as a glymphatic function index remains theoretical, as it has not yet been rigorously validated by pathophysiological studies and may be confounded by various factors, such as adjacent WM alterations or vascular signals [8, 47]. Therefore, DTI-ALPS should be interpreted with caution and always considered in the context of the underlying pathophysiology. In mood disorders, previous studies suggested that AQP4-a water channels are crucial elements of the glymphatic system- is involved in the neurobiology of mood disorders through various mechanisms [48]. In addition, another study suggested the decreased coupling strength of global blood-oxygen-level-dependent (gBOLD) signals and CSF inflow dynamics, another in-vivo MRI measurement for glymphatic function, in patients with depressive disorder, further supporting the hypothesis of glymphatic dysfunction as an early pathophysiology in mood disorder [49]. Furthermore, lithium has been found to affect the circadian rhythm of the choroid plexus, a cerebral component that significantly influences overall glymphatic function through the production of CSF in brain [50]. Bravi [51] demonstrated that an increase in choroid plexus volume in patients with BD was correlated with circulating inflammatory cytokines. Our findings, combined with previous evidence, suggested that glymphatic dysfunction might be involved in the early pathophysiology in BD and have the potential to serve as one novel treatment target. Interestingly, in subgroup analyses, we observed a significant reduction in DTI-ALPS in mixed-phase patients compared with healthy controls, whereas no significant differences were detected for the manic or depressive subgroups. These findings should be interpreted cautiously, given the limited sample sizes, particularly in the manic sub-group ($n = 11$), which constrain statistical power. Yet, despite similar sample sizes in the mixed-phase ($n = 40$) and depressive ($n = 57$) subgroups, only the mixed-phase group presented a significantly reduced DTI-ALPS values compared to healthy controls, raising the possibility of a phase-related effect. Nevertheless, due to the sample size and design limitations, we cannot draw any definitive conclusions regarding phase-specific effects. Larger-scale, longitudinal studies are essential to further explore this preliminary finding.

We also found that decreased DTI-ALPS was related to higher FW and lower FA-t values in some specific WM regions in BD. This is consistent with the findings from studies in various conditions, including older adults with metabolic syndrome [52] and the patients with cerebral small vessel disease [53]. Multiple studies have suggested that inflammatory dysregulation in the brain is involved in the pathogenesis of BD [2, 3, 54]. In addition, FW has frequently been reported to increase in BD and correlate with peripheral inflammatory markers in BD [17, 19, 21]. Thus, although elevated FW may also reflect other pathological processes, such as vasogenic edema or neurodegeneration, in the present study focusing on early-stage BD, cerebral FW is considered an in-vivo imaging marker of neuroinflammation. The observed association between the decreased DTI-ALPS and increased FW may indicate the impaired clearance and subsequent accumulation of inflammatory factors in the brain. This speculation warrants validation in future studies using more specific imaging markers or pathological confirmation. In addition, we found that lower DTI-ALPS values were associated with reduced FA-t values in several WM regions. Note that, these WM regions showing a DTI-ALPS related reduction in FA-t were highly overlapped with and were markedly smaller than those of FW values. This suggests that the accumulation of FW, potentially reflecting neuroinflammatory or fluid-related processes, emerge earlier or more diffusely than microstructural changes detectable with FA-t. One possible interpretation is that impaired perivascular fluid dynamics could contribute to persistent neuroinflammation, which over time may be linked to microstructural tissue damage. However, it is important to emphasize that all measures in this study were derived from a single-shell, relatively low-resolution diffusion sequence. Consequently, they lack pathological specificity and are limited in their ability to fully disentangle contributions from distinct processes. In addition, the estimates may be affected by partial-volume effects near CSF spaces and by the presence of crossing fibbers within a voxel. Therefore, these associations should be regarded as preliminary and require validation in future studies with higher-resolution, multi-shell data.

By contrast to the WM, we did not observe significant associations between the DTI-ALPS index and cortical GM changes. This could be explained by the methodological underpinnings of the DTI-ALPS approach, which is derived from diffusivity in deep periventricular WM along putative perivascular pathways. Thus, DTI-ALPS may provide an approximate measure of glymphatic function in the regional WM regions rather than cortical. Moreover, cortical analyses were limited by our diffusion protocol (single-shell, $b = 1000$ s/mm^2, 3-mm isotropic), where FW estimates are highly vulnerable to partial-volume effects from CSF. Finally, because our cohort consisted of drug-naïve, first-episode patients, cortical changes were expected to be subtle at this early stage. Taken together, these methodological and population factors likely explain why cortical alterations and associations with DTI-ALPS were not observed in the present study.

We found that decreased DTI-ALPS values related with lower cognitive and social abilities. This relationship between cognitive domain in executive function and DTI-ALPS is mediated by FW accumulation across widespread WM regions, including the forceps minor, right inferior fronto-occipital fasciculus, left inferior longitudinal fasciculus, right uncinate fasciculus, and bilateral anterior thalamic radiation. These tracts are known to support executive function in young adults, which may explain why increased FW within these regions mediated the observed relationship between DTI-ALPS and executive performance [55, 56]. By contrast, we did not find a mediation effects of WM microstructure damage between DTI-ALPS and social abilities. This could be explained by the characteristics of our study population, which consists of patients with first-diagnosed, drug-naïve BD. Although several WM bundles showed susceptible to decreased DTI-ALPS values, the extent of damage might remain minimal in

the early stages of the disease, potentially insufficient to affect clinical characteristics. While this finding also suggested that the FW index may serve as a more effective marker than FA-t index for monitoring disease progression in the early-stage of BD, future studies with long-term follow-up are required.

The present study had some limitations. First, the data were taken from first diagnosed, drug-naive patients, suggesting that alterations reflected by the DTI-ALPS index appear in the early stage of BD; however, there is still a lack of data on the very early or preclinical stages of BD, and a lack of follow-up results during the natural course of the disease or after medication. Therefore, more comprehensive data are needed to identify alterations in the DTI-ALPS index as a stable pathological phenomenon in BD and to determine its causal association with the onset and remission of BD. Second, DTI-ALPS, while exhibiting substantial correlation with glymphatic clearance rates as quantified by invasive MRI methodologies incorporating intrathecal gadolinium administration, fundamentally delineates diffusivity along perivascular spaces. This diffusivity, however, may not be exclusive to perivascular pathways but potentially emanate from diverse compartments, including parenchymal tissue and intravascular spaces [7, 9]. Moreover, this index was only measured at the lateral ventricle body [7], while glymphatic changes occur throughout the entire brain. As a result, DTI-ALPS can only provide an approximate measure of glymphatic function in a specific brain region. To validate our findings, future research should employ more reliable and comprehensive methods to assess glymphatic function across the whole brain. Third, we only used the FW index as a proxy for neuroinflammation in present study. The FW compartment is isotropic with a consistent diffusion coefficient in all directions, which can model the unrestricted diffusion of water molecules in the extracellular space and could be caused by neuroinflammation, atrophy, or cerebral oedema [18]. Since cerebral atrophy and oedema are unusual in adolescents and young adults, we only considered FW as a proxy for neuroinflammation here [18, 57]. Nevertheless, caution is required to interpret FW accumulation in this study strictly as neuroinflammation. Subsequent studies employing PET imaging specific to microglial activation or translocator protein could facilitate accurately assessing cerebral neuroinflammation levels, thereby validating our findings. Finally, because our diffusion data were acquired with relatively large voxels, partial-volume effects may confound these diffusion-derived measures, particularly in the cortex where FW estimates are highly vulnerable to CSF contamination. Future studies with higher-resolution diffusion acquisitions will be needed to assess cortical alterations more accurately in BD.

To conclude, our study demonstrated the lower DTI-ALPS values may increase the risk of BD. Lower DTI-ALPS indices observed in first-diagnosed, drug-naïve BD patients, were associated with localized FW accumulation, WM disintegration, and clinical deficits. These findings suggested that the decrease of DTI-ALPS could be involved in the early-stage of BD and might contribute to clinical deficits through extracellular FW accumulation, indicating an interaction between glymphatic dysfunction and neuroinflammation in BD pathophysiology. Further evidence is needed to substantiate this interpretation.

DATA AVAILABILITY

The data that support the findings of this study are available from the corresponding author upon reasonable request. All statistical code can be made available upon request by contacting: zhuohuichen0102@foxmail.com.

REFERENCES

1. Goes FS. Diagnosis and management of bipolar disorders. BMJ. 2023;381:e073591.
2. Schlaaff K, Dobrowolny H, Frodl T, Mawrin C, Gos T, Steiner J, et al. Increased densities of T and B lymphocytes indicate neuroinflammation in subgroups of schizophrenia and mood disorder patients. Brain Behav Immun. 2020;88:497–506.
3. Rao JS, Harry GJ, Rapoport SI, Kim HW. Increased excitotoxicity and neuroinflammatory markers in postmortem frontal cortex from bipolar disorder patients. Mol Psychiatry. 2010;15:384–92.
4. Zhou Y, Cai J, Zhang W, Gong X, Yan S, Zhang K, et al. Impairment of the glymphatic pathway and putative meningeal lymphatic vessels in the aging human. Ann Neurol. 2020;87:357–69.
5. Yan T, Qiu Y, Yu X, Yang L. Glymphatic dysfunction: a bridge between sleep disturbance and mood disorders. Front Psychiatry. 2021;12:658340.
6. Iliff JJ, Wang M, Liao Y, Plogg BA, Peng W, Gundersen GA, et al. A paravascular pathway facilitates CSF flow through the brain parenchyma and the clearance of interstitial solutes, including amyloid beta. Sci Transl Med. 2012;4:147ra111.
7. Taoka T, Masutani Y, Kawai H, Nakane T, Matsuoka K, Yasuno F, et al. Evaluation of glymphatic system activity with the diffusion MR technique: diffusion tensor image analysis along the perivascular space (DTI-ALPS) in Alzheimer's disease cases. Jpn J Radio. 2017;35:172–8.
8. Taoka T, Ito R, Nakamichi R, Nakane T, Kawai H, Naganawa S. Diffusion tensor image analysis ALong the perivascular space (DTI-ALPS): revisiting the meaning and significance of the method. Magn Reson Med Sci. 2024;23:268–90.
9. Zhang W, Zhou Y, Wang J, Gong X, Chen Z, Zhang X, et al. Glymphatic clearance function in patients with cerebral small vessel disease. Neuroimage. 2021;238:118257.
10. Yang C, Tian S, Du W, Liu M, Hu R, Gao B, et al. Glymphatic function assessment with diffusion tensor imaging along the perivascular space in patients with major depressive disorder and its relation to cerebral white-matter alteration. Quant Imaging Med Surg. 2024;14:6397–412.
11. Tu Y, Fang Y, Li G, Xiong F, Gao F. Glymphatic system dysfunction underlying schizophrenia is associated with cognitive impairment. Schizophr Bull. 2024;50:1223–31.
12. Li X, Ruan C, Zibrila AI, Musa M, Wu Y, Zhang Z, et al. Children with autism spectrum disorder present glymphatic system dysfunction evidenced by diffusion tensor imaging along the perivascular space. Medicine (Baltim). 2022;101:e32061.
13. Dai X, Gao L, Zhang J, Li X, Yu J, Yu L, et al. Investigating DTI-ALPS index and its association with cognitive impairments in patients with alcohol use disorder: A diffusion tensor imaging study. J Psychiatr Res. 2024;180:213–8.
14. Davies NM, Holmes MV, Davey Smith G. Reading Mendelian randomisation studies: a guide, glossary, and checklist for clinicians. BMJ. 2018;362:k601.
15. Davey Smith G, Hemani G. Mendelian randomization: genetic anchors for causal inference in epidemiological studies. Hum Mol Genet. 2014;23:R89–98.
16. Chen Z, Wang X, Teng Z, Huang J, Mo J, Qu C, et al. A comprehensive assessment of the association between common drugs and psychiatric disorders using Mendelian randomization and real-world pharmacovigilance database. EBioMedicine. 2024;107:105314.
17. Lesh TA, Maddock RJ, Howell A, Wang H, Tanase C, Daniel Ragland J, et al. Extracellular free water and glutathione in first-episode psychosis-a multimodal investigation of an inflammatory model for psychosis. Mol Psychiatry. 2021;26:761–71.
18. Pasternak O, Sochen N, Gur Y, Intrator N, Assaf Y. Free water elimination and mapping from diffusion MRI. Magn Reson Med. 2009;62:717–30.
19. Cetin-Karayumak S, Lyall AE, Di Biase MA, Seitz-Holland J, Zhang F, Kelly S, et al. Characterization of the extracellular free water signal in schizophrenia using multi-site diffusion MRI harmonization. Mol Psychiatry. 2023;28:2030–8.
20. Di Biase MA, Zalesky A, Cetin-Karayumak S, Rathi Y, Lv J, Boerrigter D, et al. Large-scale evidence for an association between peripheral inflammation and white matter free water in schizophrenia and healthy individuals. Schizophr Bull. 2021;47:542–51.
21. Tuozzo C, Lyall AE, Pasternak O, James ACD, Crow TJ, Kubicki M. Patients with chronic bipolar disorder exhibit widespread increases in extracellular free water. Bipolar Disord. 2018;20:523–30.
22. Ji F, Pasternak O, Liu S, Loke YM, Choo BL, Hilal S, et al. Distinct white matter microstructural abnormalities and extracellular water increases relate to cognitive impairment in Alzheimer's disease with and without cerebrovascular disease. Alzheimers Res Ther. 2017;9:63.
23. Mitchell T, Lehericy S, Chiu SY, Strafella AP, Stoessl AJ, Vaillancourt DE. Emerging neuroimaging biomarkers across disease stage in parkinson disease: a review. JAMA Neurol. 2021;78:1262–72.
24. Hamilton M. A rating scale for depression. J Neurol Neurosurg Psychiatry. 1960;23:56–62.
25. Young RC, Biggs JT, Ziegler VE, Meyer DA. A rating scale for mania: reliability, validity and sensitivity. Br J Psychiatry. 1978;133:429–35.

26. Sheehan DV, Harnett-Sheehan K, Raj BA. The measurement of disability. Int Clin Psychopharmacol. 1996;11:89–95.
27. Perianez JA, Lubrini G, Garcia-Gutierrez A, Rios-Lago M. Construct validity of the stroop color-word test: influence of speed of visual search, verbal fluency, working memory, cognitive flexibility, and conflict monitoring. Arch Clin Neuropsychol. 2021;36:99–111.
28. Tournier JD, Smith R, Raffelt D, Tabbara R, Dhollander T, Pietsch M, et al. MRtrix3: A fast, flexible and open software framework for medical image processing and visualisation. Neuroimage. 2019;202:116137.
29. Smith SM, Jenkinson M, Woolrich MW, Beckmann CF, Behrens TE, Johansen-Berg H, et al. Advances in functional and structural MR image analysis and implementation as FSL. Neuroimage. 2004;23:S208–219.
30. Schilling KG, Blaber J, Huo Y, Newton A, Hansen C, Nath V, et al. Synthesized b0 for diffusion distortion correction (Synb0-DisCo). Magn Reson Imaging. 2019;64:62–70.
31. Tustison NJ, Avants BB, Cook PA, Zheng Y, Egan A, Yushkevich PA, et al. N4ITK: improved N3 bias correction. IEEE Trans Med Imaging. 2010;29:1310–20.
32. Mori S, Oishi K, Jiang H, Jiang L, Li X, Akhter K, et al. Stereotaxic white matter atlas based on diffusion tensor imaging in an ICBM template. Neuroimage. 2008;40:570–82.
33. Muthuraman M, Fleischer V, Kroth J, Ciolac D, Radetz A, Koirala N, et al. Covarying patterns of white matter lesions and cortical atrophy predict progression in early MS. Neurol Neuroimmunol Neuroinflamm. 2020;7:e681.
34. Coalson TS, Van Essen DC, Glasser MF. The impact of traditional neuroimaging methods on the spatial localization of cortical areas. Proc Natl Acad Sci USA. 2018;115:E6356–E6365.
35. Huang SY, Ge YJ, Ren P, Wu BS, Gong W, Du J, et al. Genome-wide association study unravels mechanisms of brain glymphatic activity. Nat Commun. 2025;16:626.
36. O'Connell KS, Koromina M, van der Veen T, Boltz T, David FS, Yang JMK. et al. Genomics yields biological and phenotypic insights into bipolar disorder. Nature. 2025;639:968–75.
37. Syvanen AC. Toward genome-wide SNP genotyping. Nat Genet. 2005;37:S5–10.
38. Guo J, Yu K, Dong SS, Yao S, Rong Y, Wu H, et al. Mendelian randomization analyses support causal relationships between brain imaging-derived phenotypes and risk of psychiatric disorders. Nat Neurosci. 2022;25:1519–27.
39. Burgess S, Butterworth A, Thompson SG. Mendelian randomization analysis with multiple genetic variants using summarized data. Genet Epidemiol. 2013;37:658–65.
40. Yao S, Zhang M, Dong SS, Wang JH, Zhang K, Guo J, et al. Bidirectional two-sample Mendelian randomization analysis identifies causal associations between relative carbohydrate intake and depression. Nat Hum Behav. 2022;6:1569–76.
41. Burgess S, Thompson SG. Interpreting findings from Mendelian randomization using the MR-Egger method. Eur J Epidemiol. 2017;32:377–89.
42. Verbanck M, Chen CY, Neale B, Do R. Detection of widespread horizontal pleiotropy in causal relationships inferred from Mendelian randomization between complex traits and diseases. Nat Genet. 2018;50:693–8.
43. Taoka T, Naganawa S. Glymphatic imaging using MRI. J Magn Reson Imaging. 2020;51:11–24.
44. Abdolizadeh A, Torres-Carmona E, Kambari Y, Amaev A, Song J, Ueno F, et al. Evaluation of the glymphatic system in schizophrenia spectrum disorder using proton magnetic resonance spectroscopy measurement of brain macromolecule and diffusion tensor image analysis along the perivascular space index. Schizophr Bull. 2024;50:1396–410.
45. Chen Y, Wang M, Su S, Dai Y, Zou M, Lin L, et al. Assessment of the glymphatic function in children with attention-deficit/hyperactivity disorder. Eur Radiol. 2023.
46. Ota M, Sato N, Nakaya M, Shigemoto Y, Kimura Y, Chiba E, et al. Relationships between the deposition of amyloid-beta and tau protein and glymphatic system activity in Alzheimer's disease: diffusion tensor image study. J Alzheimers Dis. 2022;90:295–303.
47. Sole-Guardia G, Li H, Willemse L, Lebenberg J, Jouvent E, Tuladhar AM. Imaging brain fluid dynamics and waste clearance involving perivascular spaces in cerebral small vessel disease. Alzheimers Dement. 2025;21:e70212.
48. Gur S, Taler M, Bormant G, Blattberg D, Nitzan U, Vaknin-Dembinsky A, et al. Lack of association between unipolar or bipolar depression and serum aquaporin-4 autoantibodies. Brain Behav Immun. 2020;88:930–4.
49. Zhang Y, Peng B, Chen S, Liang Q, Zhang Y, Lin S, et al. Reduced coupling between global signal and cerebrospinal fluid inflow in patients with depressive disorder: A resting state functional MRI study. J Affect Disord. 2024;354:136–42.
50. Liska K, Dockal T, Houdek P, Sladek M, Luzna V, Semenovykh K, et al. Lithium affects the circadian clock in the choroid plexus - A new role for an old mechanism. Biomed Pharmacother. 2023;159:114292.
51. Bravi B, Melloni EMT, Paolini M, Palladini M, Calesella F, Servidio L, et al. Choroid plexus volume is increased in mood disorders and associates with circulating inflammatory cytokines. Brain Behav Immun. 2024;116:52–61.
52. Andica C, Kamagata K, Takabayashi K, Kikuta J, Kaga H, Someya Y, et al. Neuroimaging findings related to glymphatic system alterations in older adults with metabolic syndrome. Neurobiol Dis. 2023;177:105990.
53. Li H, Jacob MA, Cai M, Kessels RPC, Norris DG, Duering M, et al. Perivascular spaces, diffusivity along perivascular spaces, and free water in cerebral small vessel disease. Neurology. 2024;102:e209306.
54. Muneer A. Bipolar disorder: role of inflammation and the development of disease biomarkers. Psychiatry Investig. 2016;13:18–33.
55. Mamiya PC, Richards TL, Kuhl PK. Right forceps minor and anterior thalamic radiation predict executive function skills in young bilingual adults. Front Psychol. 2018;9:118.
56. Canales-Rodriguez EJ, Pomarol-Clotet E, Radua J, Sarro S, Alonso-Lana S, Del Mar Bonnin C, et al. Structural abnormalities in bipolar euthymia: a multicontrast molecular diffusion imaging study. Biol Psychiatry. 2014;76:239–48.
57. Hedman AM, van Haren NE, Schnack HG, Kahn RS, Hulshoff Pol HE. Human brain changes across the life span: a review of 56 longitudinal magnetic resonance imaging studies. Hum Brain Mapp. 2012;33:1987–2002.

ACKNOWLEDGEMENTS

We thank all the patients who served as research participants. We would like to thank Editage (www.editage.com) for English language editing.

AUTHOR CONTRIBUTIONS

ZC, ZT, DY and HL conceived and designed the study. ZC and ZT drafted the manuscript. JC, DY and HL revised the survey and design. YQ, SL, XX, MY, DY and JC participated in the data collection. All the authors have read and approved the final version of this manuscript.

FUNDING

This study was supported by the Interdisciplinary Direction Cultivation Project of Hunan University of Chinese Medicine (grant no. 2025JC0103), National Natural Science Foundation of China (grant no. 81971258) and the Foundation for the Integration of Chinese Excellent Traditional Culture and Modern Psychology - Project of Taoism and Mental Health Research Center, Central South University.

COMPETING INTERESTS

The authors declare no competing interests.

ETHICS APPROVAL AND CONSENT TO PARTICIPATE

All procedures involving human subjects/patients were approved by the Ethics Committee of the Second Xiangya Hospital of Central South University (approval number: 2018-067).

CONSENT FOR PUBLICATION

Our manuscript did not contain any individual person's data.

ADDITIONAL INFORMATION

Supplementary information The online version contains supplementary material available at https://doi.org/10.1038/s41398-025-03753-1.

Correspondence and requests for materials should be addressed to Zhuohui Chen, Dong Yang or Hao Li.